Heliyon 5 (2019) e02817

Contents lists available at ScienceDirect

Heliyon

journal homepage: www.heliyon.com

Heliyon

Research article

Polygonum odoratum essential oil inhibits the activity of mushroom derived tyrosinase

Anne Frances Murray [a,*], Hiroki Satooka [a], Kuniyoshi Shimizu [c], Warinthorn Chavasiri [b], Isao Kubo [a]

[a] Department of Environmental, Policy and Management, University of California, Berkeley, CA, 94720, USA
[b] Natural Products Research Unit, Department of Chemistry, Faculty of Science, Chulalongkorn University, Bangkok, 10330, Thailand
[c] Department of Agro-environmental Sciences, Faculty of Agriculture, Kyushu University, Fukuoka, Japan

ARTICLE INFO

Keywords:
Food science
Food technology
Biochemistry
Biotechnology
Plant biology
Natural products
Enzyme inhibition
Mushroom tyrosinase
Polygonum odoratum
Food preservation

ABSTRACT

Plant derived compounds are a source of long term research focus due to their applications in a variety of fields, particularly food preservation. One key way in which phytochemicals are crucial in this area is by disrupting enzyme functionality. In this work, essential oil was extracted by steam distillation from the fresh leaves of *Polygonum odoratum* (Polygonaceae), commonly known as Vietnamese coriander, and shown to effectively inhibit the oxidation of L-3,4-dihydroxyphenylalanine (L-DOPA) catalyzed by mushroom tyrosinase (EC1.14.18.1). Using GC-MS analysis, twenty five compounds were identified in the essential oil. The most abundant compounds in the essential oil were Alkanals - dodecanal (55.49%), and decanal (11.57%) - followed by anisaldehyde (6.35%); these compounds were individually investigated for inhibitory activity by performing single-compound screening. Each of the top three most abundant compounds inhibited the tyrosinase-catalyzed oxidation of L-DOPA, as identified by UV-VIS spectroscopy and oxygen consumption assays. The inhibitory activity of the major compounds increased when pre-incubated with tyrosinase and without significant additional oxygen consumption, suggesting k_{cat}-type inactivation is not involved. Interactions of the head and tail components of the major alkanals may disrupt the tertiary structure of the enzyme, presenting a potential inhibitory mechanism.

1. Introduction

Plant derived compounds play a key role in food science technologies. To identify new candidate compounds we will investigate plant sources that have established uses as homeopathic remedies. Vietnamese coriander (*Polygonum odoratum*) is a south-east Asian herb (Sakunpak et al., 2015) with homeopathic medicinal qualities (Fujita et al., 2015) including the treatment of stomach pains (Corlett et al., 2003), acting as an anti-inflammatory and has also been shown to have anti-bacterial activity (Ayaz et al., 2015; Ayaz et al., 2016; Ayaz et al., 2017). Additionally, *P. ordoratum* plant extracts are known to have high levels of antioxidant compounds. The leaves of the perennial herb are pointed with distinctive purple bands in the center of the green leaves (Shavandi et al., 2015). Interestingly, when exposed to air the leaf of *P. odoratum* does not brown, which typically occurs due to the formation of the polymer melanin (Kim and Uyama, 2005). This suggests that the compounds in *P. odoratum* may have the potential to prevent melanin production (melanogenesis). Identification of an effective melanogenesis inhibitor has important food science applications such as extending the shelf-life of fresh foods and reducing food waste (Gomez-Gullien and Martinez-Alvarez, 2005). The enzyme responsible for initiating melanin production is tyrosinase (EC 1.14.18.1), a type III copper containing oxidase (Ramsden and Riley, 2014). The active site of tyrosinase contains two copper ions coordinated by histidine residues (Olivares and Solano, 2009). Tyrosinase catalyzes the first two reactions of the melanin formation pathway. In the first of these steps, the mono-phenol L-tyrosine is ortho-hydroxylated to form an ortho-diphenol, L-DOPA (L-3,4 dihydroxyphenylalanine). In the second step, tyrosinase oxidizes L-DOPA to dopaquinone (Satooka and Kubo, 2011). Then, through a series of non-enzymatic reactions a stable intermediate, dopachrome is formed. Lastly, through oxidation and polymerization steps the pigment melanin is formed. Due to its central role in melanogenesis, tyrosinase inhibitors are expected to prevent melanin formation. In this work, we investigate the raw extract and the major compounds of *P. odoratum* essential oil as melanogenesis inhibitors. Gas chromatography-mass spectroscopy (GC-MS) of the extract revealed that 73% of the compounds present were

* Corresponding author.
E-mail address: afmurray@berkeley.edu (A.F. Murray).

https://doi.org/10.1016/j.heliyon.2019.e02817
Received 29 January 2018; Received in revised form 4 October 2019; Accepted 5 November 2019

aldehydes, with the three most prevalent compounds being dodecanal, decanal, and anisaldehyde. Previous works have identified anisaldehyde as a strong tyrosinase inhibitor (Ha et al., 2005) however the major alkanals decanal and dodecanal to the best of our knowledge have not been reported as a tyrosinase or melanogenesis inhibitors. Our objective is to quantify the efficacy of these alkanal compounds as tyrosinase inhibitors. We hypothesize that the essential oil and major alkanals in the essential oil of *P. odoratum* will inhibit tyrosinase activity. The successful identification of a new natural product source with the ability to inhibit tyrosinase functionality would present opportunities in prevention of browning in food preservation.

2. Results

2.1. Essential oil

Initial screening of the essential oil (EO) included both UV-Vis absorption, monitoring dopachrome formation, and oxygen consumption assays, following enzyme activity. The UV-Vis absorption and oxygen consumption assays revealed that 50 μg/mL EO inhibited the oxidation of L-DOPA (9% reduction in absorption relative to control) compared to vehicle treatment (Fig. 1a). Increasing the concentration of the essential oil to 100 μg/mL, and subsequently to 200 μg/mL, significantly suppressed both dopachrome formation and the oxygen consumption by 18 % and 35 %, respectively (Fig. 1a). Solubility issues above 200 μg/mL prevented testing at higher concentrations. A 10-minute pre-incubation of EO with tyrosinase significantly enhanced inhibitory efficacy for each concentration when measuring UV-Vis (Fig. 1a). In contrast, oxygen consumption assays performed after preincubation showed only an incremental increase in the inhibitory activity (Fig. 1b). The inhibitory activity of the essential oil suggests that one or more of the constituent compounds may be an effective inhibitor. The native substrate of tyrosinase, L-tyrosine, was also examined since the hydroxylation of the amino acid is the first step in the melanogenesis pathway. The essential oil showed poor inhibitory activity at 50 μg/mL. The presence of the essential oil at 100 μg/mL reduced enzyme activity by 15 % (Fig. 2). This level of inhibition was comparable to the L-DOPA results.

2.2. Major alkanals: dodecanal and decanal

The composition of the essential oil was determined using GC-MS with the list of identified compounds provided in Table 1. The three most prevalent compounds in the EO were identified as dodecanal (55.49 %, **1**), decanal (11.57 %, **2**) and anisaldehyde (6.35 %, **3**). Inhibition assays performed with an L-DOPA substrate at 250 μM dodecanal showed significant inhibition of enzyme activity in both UV-Vis and oxygen assays by 23% (Fig. 3a). At higher concentrations of 500 μM and 1000 μM there was a further significant reduction in dopachrome formation (UV-

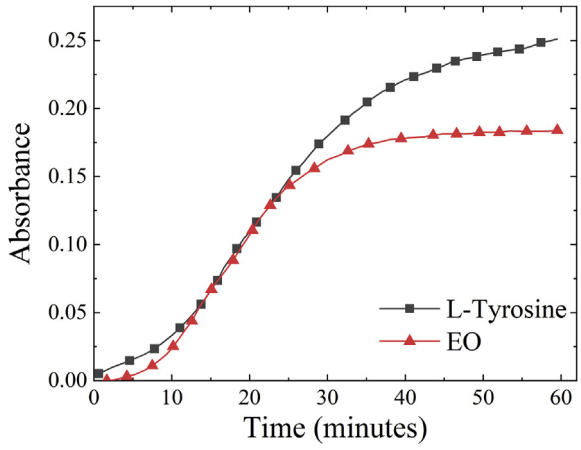

Fig. 2. Oxygen consumption of the oxidation of 500 μM of L-tyrosine and essential oil at 100 μg/mL.

Table 1
GC-MS determined composition of essential oil from *P.odoratum*.

RT	Compounds	% content
30.16	Dodecanal	55.49
19.39	*n*-Decanal	11.57
65.8	Pentacosane	7.26
18.29	*p*-Anis aldehyde	6.35
33.58	*n*-Dodecanol	3.3
63.23	2*E*-Dodecenal	2.5
31.94	*α*-Humulene	2.41
39.42	Humulene epoxide II	1.51
24.85	Undecanal	1.31
23.26	*n*-Decanol	1.13
38.17	allo-Aromadendrene epoxide	1.08
65.45	2*E*-Tridecenal	1.07
37.73	Methyl vanillin	0.86
40.58	Zierone	0.6
28.53	*n*-Undecanol	0.56
59.53	neoiso-Menthol	0.45
43.1	4-methylhexyl-2-methylbutyrate	0.43
42.53	*β*-Bisabolol	0.41
46.25	Drimenol	0.39
39.93	Tetradecanal	0.34
64.19	Triacontane	0.33
35.13	*β*-Panasinsene	0.33
13.66	*n*-Decane	0.26
11.48	3-Methyl-4-heptanone	0.05
52.14	Polygodial	0.01

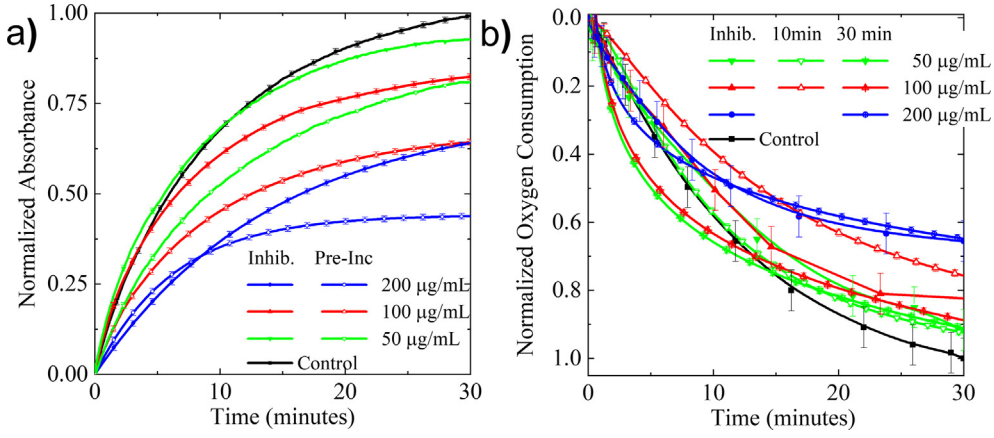

Fig. 1. UV-Vis absorption at 475 nm (**a**) and oxygen consumption (**b**) of 500 μM of L-DOPA with tyrosinase with essential oil (50 μg/mL, 100 μg/mL, 200 μg/mL).

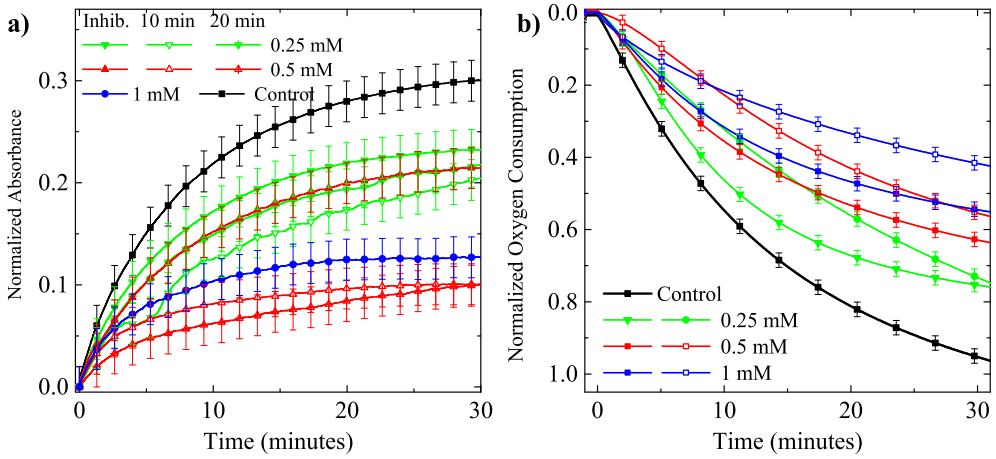

Fig. 3. UV-Vis absorption at 475 nm (**a**) oxygen consumption (**b**) of 500 μM of L-DOPA with tyrosinase dodecanal at 250 μM, 500 μM, 1 mM.

Vis absorption) by 30% and 57% respectively and oxygen consumption by 36% and 43% (Fig. 3b). A pre-incubation period of 10 min increased the inhibitory activity of dodecanal compared to the inhibition assays.

However, for the 250 μM assay, the activity recovered to become comparable to the non-incubated samples over the measurement period of 30 min. An additional 10-minute incubation (20 min total) further improved dodecanal activity (Fig. 3a). The inhibitory activity of dodecanal (500 μM) on the native L-tyrosine substrate showed suppression of activity by 8% (Fig. 4).

Decanal was the second most abundant compound (11.56%; 74.17 μM, **2**) in the essential oil. At concentrations of 125 μM there was no notable suppression of dopachrome formation, while at 250 μM and 500 μM there was significant suppression by 24% and 28%, respectively (Fig. 5). A pre-incubation period of 10 min significantly increased the inhibitory activity to 10%, 34% and 63% when measuring dopachrome formation at the same concentration. While oxygen consumption decreased by 11%, 33% and 36% at decanal concentrations of 250 μM, 500 μM and 1 mM, respectively. Interestingly, despite the significant improvement observed in the UV-Vis measurements, there was little effect of pre-incubation on oxygen consumption, with a difference of less than 9%. The only significant difference between the decanal and dodecanal is the side-chain length, suggesting the tail length plays a crucial role in determining the inhibitory activity.

The inhibitory activity of decanal was investigated using L-tyrosine as an alternative substrate. At 500 μM decanal suppressed enzyme activity by 11% when measuring oxygen consumption. The lag phase observed in L-tyrosine assays was not extended or curtailed (Fig. 6). The binding activity of dodecanal and decanal at the enzyme active site was investigated using fluorescence spectroscopy. We used the compound *N*-Phenyl-1-naphthylamine (1-NPN) since it strongly fluoresces in hydrophobic environments (Yin & others 2015). The active site in tyrosinase is hydrophobic but there are other hydrophobic regions within the tetramer subunits (Ismaya et al., 2011). In the presence of L-DOPA, tyrosinase reconfigures to expose the hydrophobic active site, which can then be occupied by either L-DOPA or 1-NPN. The control measurements show an increase in fluorescence signal, consistent with 1-NPN being present at the active site. Once the alkanals are introduced, the fluorescence signal decreases continuously with time, suggesting the hydrophobic active site is now occupied by the inhibitors. At a concentration of 500 μM there was a significant decrease in fluorescence of 80% for dodecanal and 50% for decanal relative to L-DOPA (Fig. 7). Similar trends and quantitatively similar suppression of the fluorescence signal suggests that, despite their difference in inhibitory efficacy, dodecanal and decanal share a common presence in the hydrophobic regions of the enzyme.

Dodecanal and decanal were both effective tyrosinase inhibitors. The third major compound investigated was anisaldehyde, present at 46.69 μM (6.35%, **3**), which has previously been reported as a strong tyrosinase inhibitor (Nitoda et al., 2007). In our testing, pre-incubation assays at 500 μM reduced enzyme activity by a significant 79% (data not shown). The common aldehyde head group shared by all the major compounds likely enables the inhibitory activity, while the tail group plays a role in determining the inhibitory efficacy. UV-Vis and oxygen consumption assays suggest the inhibitory binding may be irreversible.

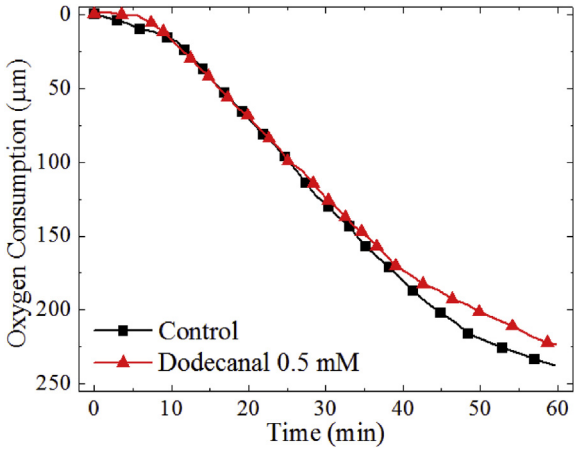

Fig. 4. Oxygen consumption of the oxidation of 500 μM of L-tyrosine and dodecanal at 500 μM.

2.3. *Shaking effects and structural analogues*

Shaking experiments were performed to investigate reversibility of the inhibitor. It is expected that, for a reversible inhibitor, agitation (shaking) will re-disperse the compounds into solution, dissociating the inhibitor from the enzyme and consequently increasing activity. A dopachrome formation assay (monitored through UV-Vis) with excess L-DOPA was initiated and at 15 min the solution was removed, quickly agitated through vortexing, and returned to the spectrophotometer. This procedure can disrupt hydrophobic interactions, and introduces oxygen to the solution, promoting further substrate oxidation if the enzyme is still active. Thus, for a reversible inhibitor with weak binding there should be an increase in enzyme activity immediately following the agitation while an irreversible inhibitor would show a much smaller increase. When measuring dopachrome formation at 475 nm the vehicle (L-DOPA) increased 0.11 absorbance units, presumably due to newly introduced oxygen, establishing a baseline recovery from the disruption. This same shaking experiment with the essential oil and dodecanal

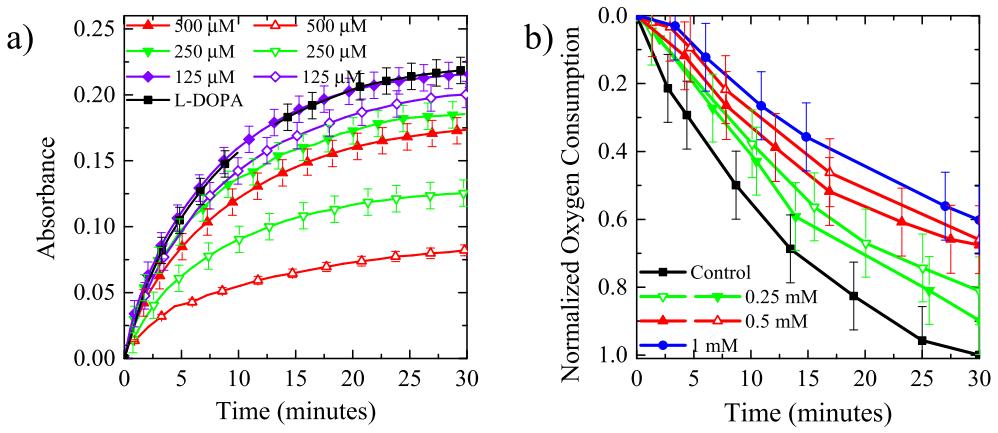

Fig. 5. UV-Vis absorption at 475 nm (**a**) oxygen consumption (**b**) of 500 µM of L-DOPA with tyrosinase decanal at 125 µM, 250 µM, 500 µM or 1 mM.

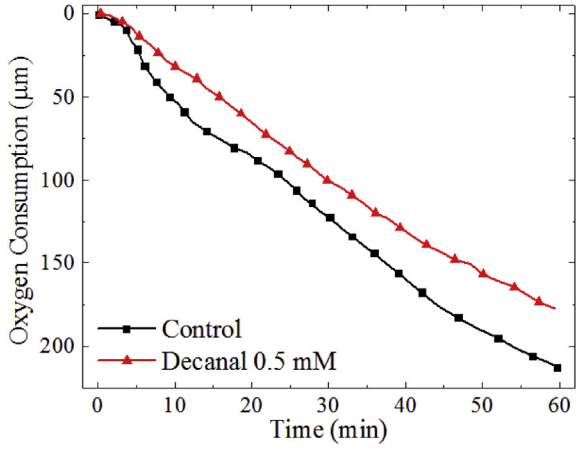

Fig. 6. Oxygen consumption of the oxidation of 500 µM of L-tyrosine and decanal at 500 µM.

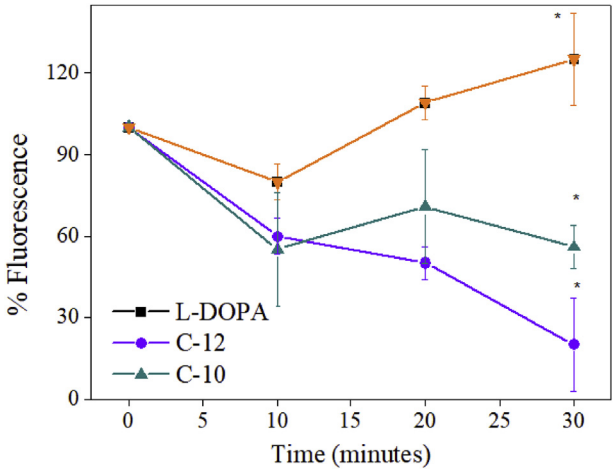

Fig. 7. Percentage fluorescence in the presence of tyrosinase and dodecanal and decanal. Asterisk indicate statistical significance ($P < 0.05$).

showed an increase in 0.10 absorbance units and 0.05 absorbance units after shaking. The recovery of the essential oil was much larger than the increase from only the introduction of oxygen, indicating that the inhibitory activity is largely reversible, while the comparatively small recovery with the dodecanal indicates irreversibility. To investigate the role of side-chain length hexanal (C6) was also tested and showed an increase in 0.10 absorbance units, which was much more than dodecanal. This indicates a positive correlation between side-chain length and inhibitory activity.

To understand the role of the alkanal side-chain, shorter chain aliphatic aldehydes down to hexanal (**7**) were investigated. Longer chain aliphatic aldehydes are uncommon as natural products, so they were not

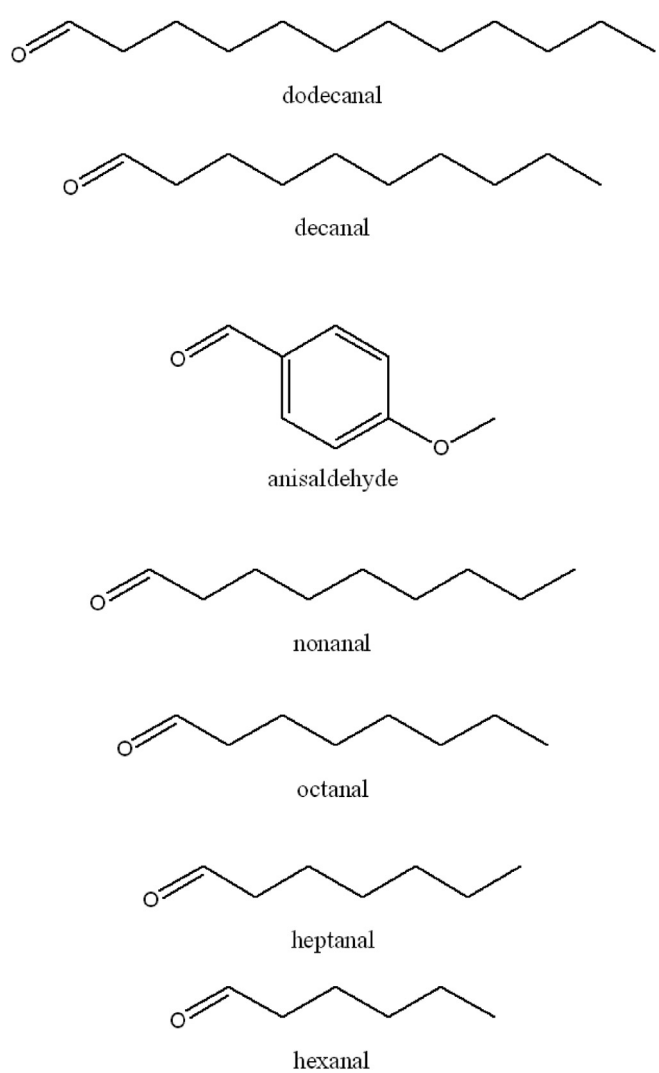

Fig. 8. Structure of dodecanal (1), decanal (2), anisaldehyde (3), nonanal (4), octanal (5), heptanal (6), hexanal (7).

examined. The saturated alkanals (**4-7**) (Fig. 8) were inhibitors of the tyrosinase catalyzed oxidation of L-DOPA. In general, pre-incubation increased alkanal activity on L-DOPA (Table 1). After 10 min of pre-incubation, compounds shorter than decanal (C10) had a lower magnitude of increasing tyrosinase inhibitory activity, suggesting that the chain length may play a role in the pre-incubation effect. Consistent with the earlier dodecanal and decanal treatments, assays performed on an L-tyrosine substrate showed weaker inhibition activity compared to those on L-DOPA. Additionally, pre-incubation with L-tyrosine (Table 2) did not improve inhibitory activity. Fluorescence measurements with 1-NPN support that these compounds significantly interact at hydrophobic sites and suggests that the alkanal side-chain length affected the activity of the enzyme.

Table 2
Alkanal inhibitory activity UV-Vis absorption at 475 nm of 500 μM of L-DOPA with tyrosinase and various alkanals at 500 μM and percentage fluorescence of alkanals on L-DOPA. Asterisk indicates values of $P < 0.05$ were considered statistically significant (*).

Compound	% Change of enzyme inhibition Pre-incubated	% Fluorescence
C6	2	89
C7	3	80
C8	5	75
C9	8	25
C10	36*	50
C12	32*	20

3. Discussion

The spectroscopy and oxygen consumption assays confirm our hypothesis that Vietnamese coriander essential oil and its major components (dodecanal, decanal, and anisaldehyde) effectively inhibit the tyrosinase catalyzed oxidation of L-DOPA. All of the major compounds have an aldehyde head group, suggesting this may be the source of the observed inhibitory activity, while the inhibitory efficacy is determined by the side chain group. The role of the side-chain group is further emphasized by comparing the inhibitory efficacy of dodecanal, decanal and hexanal. Shaking experiments support the irreversible inhibitory activity of dodecanal efficacy.

In a possible inhibitory mechanism, the aldehyde head group quickly binds at hydrophobic sites on the enzyme, and then the aliphatic tail group disrupts the enzyme tertiary structure through hydrophobic interactions. The tyrosinase active site in particular has been previously suggested to be susceptible to inhibitory molecules, following binding by a Schiff base formation, a non-competitive mechanism (Kubo and Kinst-Hori, 1998). Specifically, the double-bound oxygen located on the aldehyde head undergoes a single-replacement with a nitrogen in the active pocket and forms a Schiff base with a primary amino group (Yokoi et al., 1990). In these previous cases the inhibitor was an alpha, beta aldehyde which is known to be more reactive than the unsaturated counterparts explored here. The Schiff base mechanism is expected to be reversible (Xavier and Srividhya, 2014) and does not consume additional oxygen from the solution, consistent with the oxygen consumption assays. Pre-incubation assays improved inhibitory activity without significantly increasing the amount of oxygen consumed. This is consistent with the above explanation but also suggests a time-dependent inhibition in which the hydrophobic side-chain requires time to bind with the enzyme and disrupt the tertiary structure. The hydrophobic portions of the enzyme include the active pocket but additionally are responsible for stabilizing the subunits of the tyrosinase tetramer (Isyama et al., 2011). Native proteins, including tyrosinase, are known to have poor conformational stability and are sensitive to hydrophobic disruptions (Gelman et al., 2013). The aldehyde head group found on the major compounds is hydrophilic, with a hydrophobic aliphatic tail, with the longer chains being more hydrophobic. At low concentrations the polar head keeps the compound dissolved as a monomer (Otzen et al., 2009). Once the concentration of the compound is increased the monomers start to associate through their hydrophobic tails to form micelles (Otzen, 2011). Thus, the reduction of dopachrome formation by the essential oil could also have been due to the interference as a surfactant-like inhibitor (Otzen, 2011). Here, we suggest an inhibitory mechanism in which the aldehyde head moiety (I) acts as a 'barb' reversibly and quickly binding to the enzyme (E) active pocket and forming an EI complex as a non-competitive inhibitor. Then slow hydrophobic interactions between the alkyl chain and the hydrophobic domain of the enzyme disrupt the enzymes' tertiary structure, reducing activity.

These results present new opportunities for effective tyrosinase inhibitors. Since the essential oil is derived from a plant source (Hunter, 1996) this could be a sustainable alternative to synthetic topical anti-browning control agents. The principle compounds investigated in this work currently have commercial uses, and this work demonstrates and expanded potential for these compounds as tyrosinase inhibitors.

4. Experimental

4.1. Materials

L-DOPA (CAS # 59-92-7), L-tyrosine (CAS # 60-18-4), dodecanal (CAS # 112-54-9), decanal (CAS # 112-31-2), and all other alkanals and dimethyl sulfoxide (DSMO) (CAS # 67-68-5) were purchased from Sigma-Aldrich (Milwaukee, MN, USA). Mushroom derived tyrosinase (CAS # 9002-10-2) was also purchased from Sigma-Aldrich and was further purified by anion-exchange chromatography using DEAE-Sepharose Fast Flow (Pharmacia, Uppsala, Sweden), as previously described (Satooka and Kubo, 2011). All measurements were made in triplicate and on separate occasions.

4.2. Collection and extraction

Fresh leaves of *P. ordoratum* were collected in the Nakhon Phatom province, Thailand in 2013. The fresh leaf material was steam distilled and essential oil collected and extracted as described in Fujita et al. (2015). The essential oil was then stored at -30 °C for further analysis.

4.3. GC-MS analysis

The essential oil of *P. odoratum* was analyzed through gas chromatography-mass spectroscopy from Fujita et al. (2015), using a GC-17A/QP5050 (Shimadzu Co., Ltd., Kyoto, Japan) with a DB-5 column (0.25 mm × 30 mm i.d. with 0.25 μm film thickness) (J & W Scientific Inc., Folsom, USA). The temperature pattern was as described: 45 °C for 8 min, followed by an increase of 2.5 °C min^{-1} to 180 °C, and 10 °C min^{-1} to 250 °C, and held there for 3 min. Additional testing settings were: an injection temperature of 250 °C, an ion source temperature of 250 °C, ionization energy of 70 eV, the carrier gas was He at 1.7 mL min^{-1}, an injection volume of 1 μL (90 μg/mL Et_2O), split ratio 1:20, and mass range m/z 50 to 450. Identification of the compounds was performed by comparison of the mass spectrum with the mass spectra database Wiley 9^{th} library and NIST08 library.

4.4. In-vitro enzyme assay

4.4.1. Spectroscopy

Photo-spectroscopy (UV-VIS) measurements were performed at 475 nm on a Shimadzu 1700 (Tokyo, Japan). This wavelength allows the identification of dopachrome. Samples were dissolved in DMSO and the final concentration of DMSO was always 3%. Inhibition assays were performed by dissolving samples in DMSO and only used for experimentation after their dilution. The final concentration of DMSO was always 3%. For inhibition assays, a test solution of 3 ml was prepared consisting of 1.95 ml distilled and filtered H_20, 0.725 ml of 67 mM phosphate buffer (pH = 6.8), 0.125 ml L-DOPA (from a 6 mM stock) were

mixed and incubated at 30 °C for 5 min. At this point, the 100 μl of the sample solution and 100 μl of the purified tyrosinase in phosphate buffer was added (1 μg/ml) to the mixture in this order. Once tyrosinase was added to the solution the absorbance was measured for 30-60 min. For pre-incubation assays 1.95 ml distilled and filtered H_20, 0.725 ml of 67mM phosphate buffer (pH = 6.8), 100 μl of the sample solution and 100 μl of the purified tyrosinase was added (1 μg/ml) and incubated for 10 min (or 20 min) at 30 °C, prior to the addition of L-DOPA. For assays testing an L-tyrosine substrate the same procedures were followed. This methodology was adapted from previously reported method (Satooka and Kubo, 2011), with a final concentration of enzyme at 1 μg/mL and kojic acid as the positive control.

4.4.2. Oxygen consumption

Oxygen consumption measurements were taken using an OBH 100 oxygen electrode with a water jacket chamber using an YSI 5300 oxygen monitor (all from Yellow Springs Instruments Co., Yellow Springs, OH). Inhibition and pre-incubation assays were preformed as described above, oxygen consumption was then monitored at 30 °C for 30 min.

4.4.3. Fluorescence

Fluorescence measurements of inhibitory activity were performed using *N*-Phenyl-1-naphthylamine (1-NPN). We followed procedures from (Yin et al., 2015) with slight modification. Measurements were performed on an EnVision Plate reader 2104i (Perkin-Elmer, Waltham, MA, USA), using a 340 nm excitation light and monitoring emissions at 460 nm. Inhibitory assay solutions were prepared as described above, with the fluorescence probe 1-NPN(20 μM) added to the solution, then the solution was incubated at 30 °C for 10 min. The 1-NPN mixtures were loaded into the wells of a 96 well plate, then the candidate inhibitor was added to this solution followed by the tyrosinase. Emissions were measured every 5 min for 30 min total. To avoid light interference, measurements were taken only after the light path way was shut for at least 10 s.

4.4.4. Statistical analysis

Data is presented as the mean and standard error mean (mean ± SEM). The data analysis was performed using a one-way-analysis of variance (ANOVA) followed by a post hoc Tukey test using R version 3.1.3. Statistical differences less than $P < 0.05$ were considered statistically significant.

Declarations

Author contribution statement

Anne F. Murray: Performed the experiments; Analyzed and interpreted the data; Wrote the paper.

Hiroki Satooka: Performed the experiments.

Kuniyoshi Shimizu, Warinthorn Chavasiri: Contributed reagents, materials, analysis tools or data.

Isao Kubo: Conceived and designed the experiments.

Funding statement

This research did not receive any specific grant from funding agencies in the public, commercial, or not-for-profit sectors.

Competing interest statement

The authors declare no conflict of interest.

Additional information

No additional information is available for this paper.

References

Ayaz, M., Junaid, M., Ullah, F., Sadiq, A., Khan, M.A., Ahmad, W., Shah, M.R., Imran, M., Ahmad, S., 2015. Comparative chemical profiling, cholinesterase inhibitions and anti-radicals properties of essential oils from Polygonumhydropiper L: a Preliminary anti- Alzheimer's study. Lipids Health Dis. 14, 141.

Ayaz, M., Junaid, M., Ullah, F., Sadiq, A., Ovais, M., Ahmad, W., Ahmad, S., Zeb, A., 2016. Chemical profiling, antimicrobial and insecticidal evaluations of Polygonumhydropiper L. BMC Complement Altern. Med. 16, 502.

Ayaz, M., Junaid, M., Ullah, F., Sadiq, A., Shahid, M., Ahmad, W., Ullah, I., Ahmad, A., Syed, 2017. GC-MS analysis and gastroprotective evaluations of crude extracts, isolated Saponins, and essential oil from polygonumhydropiper L. Front. Chem. 5, 58.

Corlett, L., Dean, E., Grivetti, L., 2013. Hmong gardens: botanical diversity in an urban setting. Econ. Bot. 57, 365–379.

Fujita, K., Chavasiri, W., Kubo, I., 2015. Anti-Salmonella activity of volatile compounds of Vietnam coriander. Phytother Res. 29, 1081–1087.

Gelman, H., Perlova, T., Gruebele, M., 2013. Dodine as a protein denaturant: the best of two worlds? J. Phys. Chem. B 117, 3090–3097.

Gomez-Gullien, M.C., Martinez-Alvrez, O., 2005. Melanosis inhibition and SO2 residual levels in shrimp Parapenaeus longirostris after different sulfite-based treatments. J. Sci. Food Agric. 85, 1143–1148.

Ha, T.J., Tamura, S., Kubo, I., 2005. Effects of mushroom tyrosinase on anisaldehyde.J. Sci. Food Agric. 53, 7024–7028.

Hunter, M., 1996. Austrilian Kesom oil – a new essential oil for the flavor and fragrance industry. Agro Food Ind. Hi-Tech 7, 26–28. ISSN:1120–6012.

Ismaya, W.T., Rozeboom, H.J., Weijn, A., Mes, J.J., Fusetti, F., Wichers, H.J., Dijkstra, B.W., 2011. Crystal structure of agaricus bisporus mushroom tyrosinase: identity of the tetramer subunits and interaction with tropolone. J. Biochem. 50, 5477–5486.

Kim, Y.J., Uyama, H., 2005. Tyrosinase inhibitors from natural and synthetic sources: structure, inhibition mechanism and perspective for the future. Cell. Mol. Life Sci. 62, 1707–1723.

Kubo, I., Kinst-Hori, I., 1998. Tyrosinase inhibitors from cumin. J. Sci. Food Agric. 46, 5338–5341.

Nitoda, T., Fan, M.D., Kubo, I., 2007. Anisaidehyde, a melanogenesis potentiator. Z. Naturforsch., C: Biosci. 62, 143–149.

Olivares, C., Solano, C., 2009. New insights into the active site strucutre and catalytic mechanism of tyrosinase and it's realted proteins. Pigment Cell Melanoma Res. 22, 750–760.

Otzen, D., 2011. Protein-surfactant interactions: a tale of many states. Biochim. Biophys. Acta 1814, 562–591.

Otzen, D.E., Sehgal, P., Westh, P., 2009. Alpha-Lactalbumin is unfolded by all classes of surfactants but by different mechanisms. J. Colloid Interface Sci. 329, 273–283.

Ramsden, C.A., Riley, P.A., 2014. Tyrosinase:The four oxidation states of the active site and their relevance to enzymatic activation, oxidation and inactivation.Bioorg. Med. Chem. 22, 2388–2395.

Sakunpak, A., Suksaeree, J., Pathompak, P., Charoonratana, T., Chankana, N., Sermkaew, N., 2015. Thin-layer chromatography—densitometry and thin-layer chromatography—image analysis for screening bile acid-binding activities of Thai edible plants. J. Planar Chromatogr. Mod. TLC 28, 380–385.

Satooka, H., Kubo, I., 2011. Effects of thymol on mushroom tyrosinase-catalyzed melanin formation. J. Sci. Food Agric. 59, 8908–8914.

Shavandi, M., Haddadian, Z., Ismail, M., 2015. Eryngium foetidum, Coriandrum sativum and Persicaria odorata: a review. J. Asian Sci. Res. 2, 410–426.

Xavier, A., Srividhya, N., 2014. Synthesis and study of schiff base ligands. J. Appl. Chem. 7, 06–15.

Yin, J., Choo, Y.M., Duan, H.X., Leal, W.S., 2015. Selectivity of odorant-binding proteins from the southern house mosquito tested against physiologically relevant ligands. Front. Physiol. 56.

Yokoi, H., Takeuchi, A., Yamada, S., 1990. Esr studies on salicyladehyde schiff base complexes of copper (III) dimer formation on Bis(N-alkylsalcylidenemination- copper (II) complexes and their derivatives in toluene. Bull. Chem. Soc. Jpn. 63, 1462–1466.